European Journal of Human Genetics (2008) 16, 1459–1466

www.nature.com/ejhg

ARTICLE

Characterization of a 7.6-Mb germline deletion encompassing the *NF1* locus and about a hundred genes in an NF1 contiguous gene syndrome patient

Eric Pasmant*[,1,2], Aurélie de Saint-Trivier[2], Ingrid Laurendeau[1], Anne Dieux-Coeslier[3], Béatrice Parfait[1,2], Michel Vidaud[1,2], Dominique Vidaud[1,2] and Ivan Bièche[1,2]

[1]*UMR745 INSERM, Université Paris Descartes, Faculté des Sciences Pharmaceutiques et Biologiques, Paris, France;* [2]*Service de Biochimie et de Génétique Moléculaire, Hôpital Beaujon AP-HP, Clichy, France;* [3]*Service de Génétique Clinique, Hôpital Jeanne de Flandre, Lille, France*

We describe a large germline deletion removing the *NF1* locus, identified by heterozygosity mapping based on microsatellite markers, in an 8-year-old French girl with a particularly severe NF1 contiguous gene syndrome. We used gene-dose mapping with sequence-tagged site real-time PCR to locate the deletion end points, which were precisely characterized by means of long-range PCR and nucleotide sequencing. The deletion is located on chromosome arm 17q and is exactly 7 586 986 bp long. It encompasses the entire *NF1* locus and about 100 other genes, including numerous chemokine genes, an attractive *in silico*-selected cerebrally expressed candidate gene (designated *NUFIP2*, for nuclear fragile X mental retardation protein interacting protein 2; NM_020772) and four microRNA genes. Interestingly, the centromeric breakpoint is located in intron 4 of the *PIPOX* gene (pipecolic acid oxidase; NM_016518) and the telomeric breakpoint in intron 5 of the *GGNBP2* gene (gametogenetin binding protein 2; NM_024835) coding a transcription factor. As *PIPOX* and *GGNBP2* have the same transcriptional orientation, we postulated, and then confirmed, the existence of a chimeric transcript. This transcript, and/or haploinsufficiency of one or several deleted genes, could explain the clinical severity of the syndrome in this patient.

European Journal of Human Genetics (2008) **16**, 1459–1466; doi:10.1038/ejhg.2008.134; published online 23 July 2008

Keywords: neurofibromatosis type 1; microdeletion; contiguous gene syndrome

Introduction

Neurofibromatosis type 1 (NF1, OMIM 162200) is an autosomal disorder[1] with estimated incidence of 1 in 3500 live births. The main features of NF1 are multiple neurofibromas, café-au-lait spots, axillary freckling, Lisch nodules, tibial pseudarthrosis, and a predisposition to certain benign and malignant tumors of the nervous system.[2]

In more than 95% of cases, NF1 is due to autosomal dominant loss-of-function mutations of the *NF1* gene (neurofibromin 1; NM_000267).[3] *NF1* is located at 17q11.2 and contains 57 translated exons distributed over ~350 kb. The protein encoded by *NF1* is a GTPase activating protein (neurofibromin) that acts as a negative regulator of the RAS-mitogen-activated protein kinase (MAPK) signaling cascade.[4] Most NF1 patients (90–95%) have a truncated mutation (point mutation, splice mutation, small deletion, insertion, or duplication). However, 5–10% of patients have a microdeletion that encompasses

***Correspondence: Dr E Pasmant, UMR745 INSERM, Université Paris Descartes, Faculté des Sciences Pharmaceutiques et Biologiques, 4 avenue de l'Observatoire, Paris 75006, France.**
Tel: +33 1 53 73 97 25; Fax: +33 1 44 07 17 54;
E-mail: eric.pasmant@etu.univ-paris5.fr
Received 6 February 2008; revised 26 May 2008; accepted 19 June 2008; published online 23 July 2008

NF1 and neighboring genes.[5] Two recurrent types (called typical *NF1* microdeletions) have been reported in most of the NF1 patients with microdeletions.[6] The type I microdeletion is interchromosomal, meiotic in origin, and 1.4 Mb long. The type II microdeletion is smaller (1.2 Mb), often occurs in patients with somatic mosaicism, and arises from a different molecular mechanism: intrachromosomal recombination during mitosis. Type I deletions are caused by nonallelic homologous recombination between paralogous sequences flanking the *NF1* gene: *NF1* proximal and distal low-copy repeats (*NF1–REP-a* and *-c*).[7] Type II breakpoints are located in the *SUZ12* gene (suppressor of zeste 12 homolog; NM_015355) and its pseudogene *SUZ12P*.[6–8] Less frequent than these two types of deletions are the so-called atypical *NF1* deletions with nonrecurring breakpoints.[9]

Here, using a two-step strategy, we identified the exact genetic rearrangement – a very large *de novo* deletion encompassing the *NF1* locus and numerous additional genes – accounting for a severe NF1 phenotype in a French patient. We used gene dose mapping with sequence-tagged site (STS) real-time PCR to locate the deletion breakpoints, and then precisely characterized them by means of long-range PCR and nucleotide sequencing. We thereby identified a deletion of 7.6 Mb encompassing the recurrent typical 1.4 and 1.2 Mb deletions.

We also determined the complete physical map and gene content (~100 genes, including four microRNA genes) within the 7.6 Mb deletion. Finally, we detected and quantified a chimeric transcript resulting from this genetic rearrangement.

Patients, materials, and methods

Patients

The family (Figure 1a) has been investigated since 2000 at Centre Hospitalier Régional Universitaire de Lille, France. There was no familial history of NF1 and no parental consanguinity.

DNA and RNA extraction

High-molecular-weight DNA was prepared by standard proteinase K digestion followed by phenol-chloroform extraction from whole-blood leukocytes. Total RNA was extracted from whole-blood leukocytes by using the acid-phenol guanidium method. The quality of the total RNA samples was determined by electrophoresis through agarose gels and staining with ethidium bromide, and the 18S and 28S RNA bands were visualized under ultraviolet light.

Mutation screening

Genomic DNA from the proband and both parents was amplified with primers specific for *PTPN11* (protein tyrosine phosphatase, nonreceptor type 11; NM_002834), *KRAS* (v-Ki-ras2 Kirsten rat sarcoma viral oncogene homolog; NM_004985), *RAF1* (v-raf-1 murine leukemia viral oncogene homolog 1; NM_002880), and *SOS1* (son of sevenless homolog 1; NM_005633) coding exons and their intron boundaries. The primer oligonucleotide sequences and PCR conditions are available on demand. PCR was performed with the Taqman PCR Core Reagent Kit (Applied Biosystems). Mutation screening was performed using bidirectional DNA sequencing of purified PCR products with the ABI BigDye terminator sequencing kit (Applied Biosystems) on an ABI Prism 3130 automatic DNA sequencer (Applied Biosystems). Sequences were aligned with Seqscape® analysis software (Applied Biosystems) and were compared with the corresponding reference sequences for genomic DNA.

Microsatellite typing

A series of 17q11.2-linked microsatellite markers were typed for segregation analysis in this family. The primer oligonucleotide sequences are available on demand. After amplification with a 5′-end-labeled primer, followed by the addition of an internal size standard (Genescan 2500-ROX: Applied Biosystems), the PCR products were separated on 6% polyacrylamide/7 M urea gel, using an ABI PRISM 310 DNA sequencer (Applied Biosystems). The results were analyzed with the Genescan 672 (version 1.2) software package.

STS real-time PCR-based gene-dose mapping

In this method, quantitative values are obtained from the threshold cycle number at which the increase in the signal associated with exponential growth of PCR products begins to be detected by Applied Biosystems analysis software, used as recommended in the manufacturer's manuals. The precise amount of genomic DNA added to each reaction mix (based on optical density) and its quality (ie, lack of extensive degradation) are both difficult to assess. We, therefore, also quantified the *ALB* gene (encoding albumin and mapping to chromosome region 4q11-q13) as an endogenous DNA control, and each sample was normalized on the basis of its *ALB* content. The relative STS marker copy number was also normalized to a calibrator, or 1 × sample, consisting of genomic DNA from a normal subject. Final results, expressed as *N*-fold differences in the target STS marker copy number relative to the *ALB* gene and the calibrator, and termed 'NSTS', were determined as follows: $\mathrm{NSTS} = 2^{(\Delta\mathrm{Ct\ sample} - \Delta\mathrm{Ct\ calibrator})}$, where ΔC_t values of the sample and calibrator are determined by subtracting the average C_t value of the target STS marker from the average C_t value of the *ALB* gene. Given the target STS marker, samples with NSTS values of 0.5 and 1.0 were considered deleted and normal, respectively. Primers for *ALB* and the 45 17q11.2-linked STS markers were chosen with the assistance of the computer program Oligo 4.0 (National Biosciences). We conducted BLASTN searches against nr (the non redundant set of the GenBank, EMBL and DDBJ

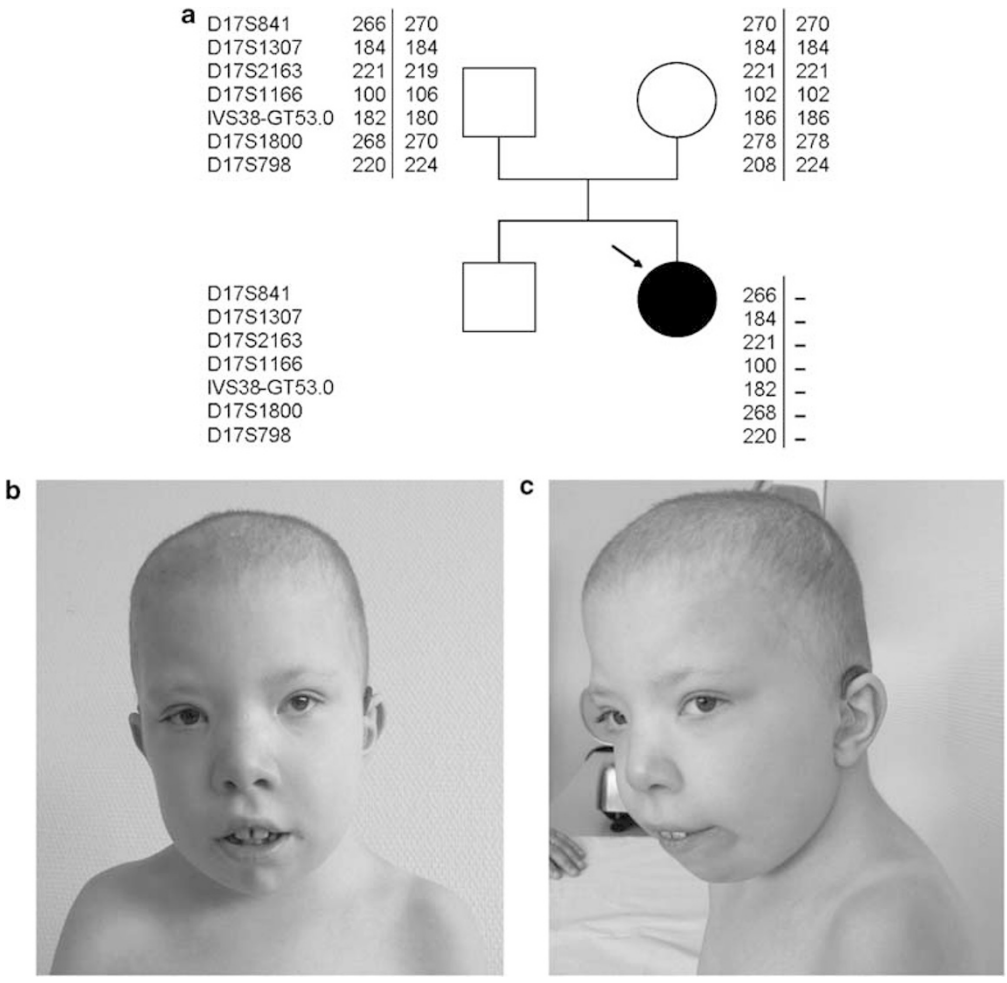

Figure 1 Family pedigree and photographs. (**a**) Haplotype reconstruction of seven microsatellite polymorphic markers at 17q11.2 (*NF1* locus) in the French NF1 family. Markers D17S1307, D17S2163, D17S1166, and IVS38-GT53.0 are located in the *NF1* gene, whereas markers D17S841, D17S1800, and D17S798 are extragenic. This marker analysis shows that the patient is hemizygous at the *NF1* locus and that the deletion occurred *de novo* and was maternal in origin. (**b**) and (**c**) Frontal and lateral views of the propositus at 8.5 years of age, showing the following dysmorphic features: high forehead with bitemporal constriction, micrognathy, hypertelorism with epicanthi, low-set and posteriorly angulated ears, strabismus, thick lips, sparse eyebrows, and short webbed neck. Written parental consent was obtained to publish the photographs.

database sequences) to confirm the total STS specificity of the nucleotide sequences chosen for the primers. The primer pairs for each STS were selected to be unique in the human genome; in particular, they were located outside repetitive DNA sequences (Alus, LINEs, and so on). All PCR reactions were performed with an ABI Prism 7900 Sequence Detection System (Applied Biosystems) and the SYBR® Green PCR Core Reagents kit (Applied Biosystems). Experiments were performed with triplicates for each data point.

Fine characterization of the 7.6-Mb germline deletion

Long-range PCR was performed with the Expand™ Long Template PCR System (Boehringer) as recommended by the manufacturer. Forward primer STS33 and reverse primer STS43 amplified a ~1.5-kb mutant genomic fragment, the normal fragment being too large (7.6 Mb) to be amplified. The 1.5-kb PCR product was sequenced as described above.

Chimeric transcript detection

Specific RT-PCR to detect the chimeric transcript was performed with forward primer CHIMERIC-U (5′-ACCACC TCCAGGAGCTACCA-3′) and reverse primer CHIMERIC-L (5′-GGATATTGTATGCTCGGAGGACT-3′) designed to hybridize to *PIPOX* exon 4 and *GGNBP2* exon 6, respectively. The RT-PCR products were sequenced as described above.

Chimeric transcript quantification with real-time RT-PCR

The theoretical and practical aspects of real-time quantitative RT-PCR using the ABI Prism 7900 Sequence Detection System (Applied Biosystems) have been described in detail

elsewhere.[10] Briefly, results, expressed as *N*-fold differences in target gene (*PIPOX, GGNBP2,* or *CHIMERIC*) expression relative to an endogenous RNA control (*TBP*), termed N_{target}, are determined with the formula: $N_{target} = 2^{\Delta C_t sample}$, where the ΔC_t value of the sample is determined by subtracting the C_t value of the target gene from the C_t value of the *TBP* gene. The N_{target} values of the samples were subsequently normalized to a 'basal mRNA level', ie, normalized to the smallest quantifiable amount of target gene mRNA (target gene C_t value = 35, and then scored as the smallest N_{target} value, ie, N_{target} value = 1). Samples with very low levels of target gene mRNA (not quantifiable in the real-time quantitative RT-PCR assay: $C_t > 35$), were considered as 'nonexpressed' (N_{target} value = 0).

The nucleotide sequences of the primers for *TBP* and for the three target genes are available on demand. To avoid amplification of contaminating genomic DNA, one of the two primers was placed at the junction between two exons. Experiments were performed with triplicates for each data point.

Bioinformatic analysis

The *in silico* sequence analysis was performed using the following database and bioinformatics tools: Ensembl (http://www.ensembl.org/index.html), UCSC Genome Bioinformatics (http://genome.ucsc.edu/), NCBI Entrez Gene (http://www.ncbi.nlm.nih.gov/sites/entrez?db=gene&cmd=search&term/), and NCBI BLAST (http://www.ncbi.nlm.nih.gov/blast/Blast.cgi). The *in silico* miRNAs target sites prediction was performed using miRBase Targets Version 5 (http://microrna.sanger.ac.uk/targets/v5/). The literature-mining bioinformatics approach to prioritize disease genes was performed using aGeneApart software (www.esat.kuleuven.be/ageneapart).

Results

Clinical report

The propositus, a girl of 8.5 years of age, was the second child of healthy nonconsanguineous parents (Figure 1a). Echography at the third trimester of pregnancy showed bilateral pleural effusion and thoracic edema. Polyhydramnios was also diagnosed. Cesarean delivery was performed during the 38th week of amenorrhea because of acute fetal distress. Postnatally, she had hypotonia, generalized edema, and bilateral chylothorax. She had poor growth and weight gain in the first year of life. Magnetic resonance imaging (MRI) of the brain performed at the age of 5 years showed several hyperintense T2-weighted lesions (unidentified bright objects) in the left and right lentiform nucleus, thalamic nuclei, peduncular region, and white substance of the cerebellum. Kidney ultrasound examination was normal. At the age of 8.5 years, she measured 115 cm (−2 SD), weighed 21 kg (−1.5 SD) and had a cranial perimeter of 53 cm (+1 SD).

The propositus had both: (i) NF1 features: café-au-lait spots appeared by the age of 7 months, multiple lentigines, subcutaneous and cutaneous neurofibromas, hyperplasia of the optic chiasma and the left optic nerve (MRI was performed at the age of 1 year), and scoliosis (corrected by a surgical corset) and (ii) severe less common NF1 features: a congenital ventricular septal defect with pulmonary valve stenosis, global hypotonia, distinct craniofacial anomalies (Figure 1b and c) including a coarse face, relative macrocephaly, a high forehead with bitemporal constriction, micrognathy, hypertelorism with epicanthi, palpebral hemangiomas, low-set and posteriorly angulated ears, strabismus, thick lips, teeth anomalies, a low posterior hairline with curly and sparse hair, sparse eyebrows, a short webbed neck and pterygium colli, sternal deformity with pectus carinatum superiorly and pectus excavatum inferiorly, articular hyperlaxity, and clinodactyly.

Her development was slow and she was severely mentally retarded: she first walked at the age of 7 years, and had mastered only a few words at the age of 8 years.

She also had generalized epileptic seizures (absences) and hearing loss. No hematological anomalies were found; in particular, the clotting time was normal.

Examination of the mother and father, who were respectively 25 and 39 years old when their daughter was conceived, showed no signs of NF1; in particular, dermatological and ophthalmologic evaluations were normal.

Molecular analysis

A standard karyotype, performed in the neonatal period, was normal (46, XX). No *PTPN11, KRAS, RAF1*, or *SOS1* coding sequence mutations were found.

Analysis of four *NF1* intragenic (D17S1307, D17S2163, D17S1166, and IVS38-GT53.0) and three extragenic (D17S841, D17S1800, and D17S798) microsatellite markers showed a hemizygous haplotype, suggesting a sporadic germline deletion removing the entire *NF1* locus (Figure 1a). To determine its precise size and end points, we estimated the number of copies (one or two) by using a three-step real-time PCR-based dosage assay for 45 STS regularly spaced within the breakpoint regions (Figure 2). We then precisely characterized the deletion breakpoints by means of long-range PCR with primers STS33-F and STS43-R (generating a PCR product of ~1.5 kb) and nucleotide sequencing. The deletion was exactly 7 586 986 bp long and was located on chromosome arm 17q between nucleotides 24 405 358 and 31 992 345 (numbered as in build 36.1 of the National Center for Biotechnology Information (NCBI)).

We then developed a simple and rapid PCR method to detect the junction fragment. Only samples from the propositus yielded a 734 bp fragment with primers JONCTION-U (5′-GAGCTGGAAGCCCGAGAGT-3′) and JONCTION-L (5′-GGTGACAATGACACAAATGAGATATT-3′). A healthy control sample yielded no PCR product, the

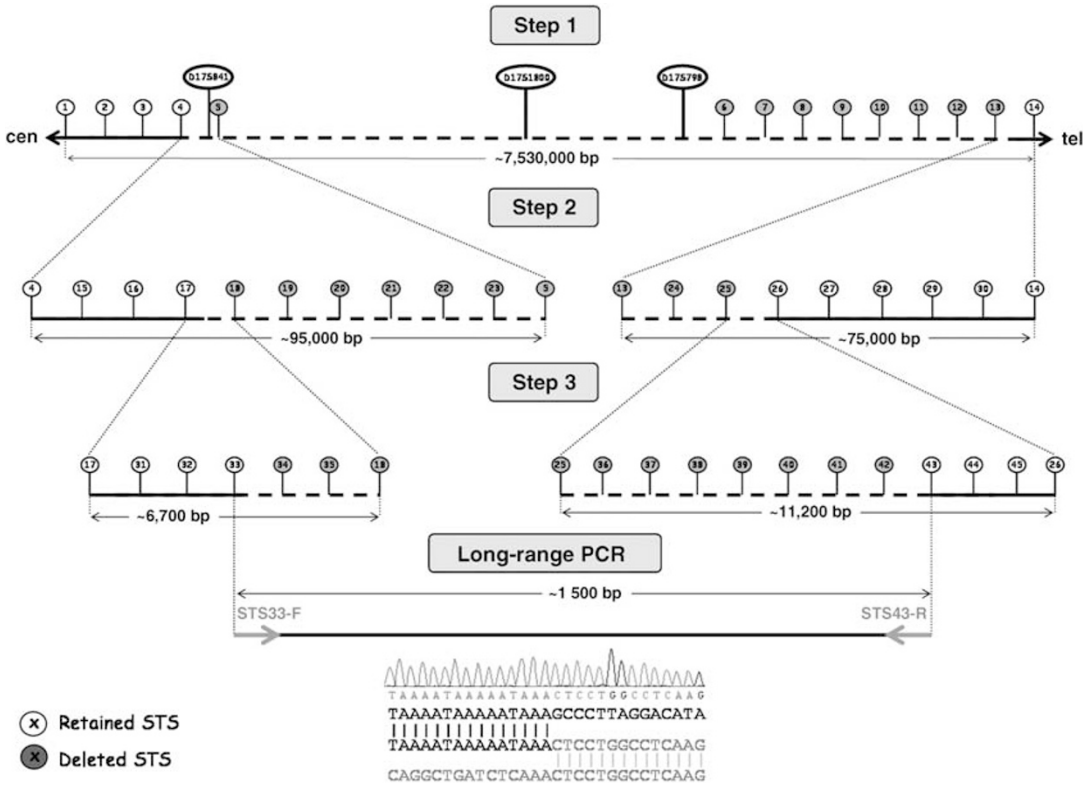

Figure 2 STS real-time PCR-based gene-dose mapping assay and genomic deletion junction-specific PCR. Multiple primers were designed to be regularly spaced every ~85 kb (step 1), ~10 kb (step 2), and ~1 kb (step 3) within breakpoint regions. Long-range PCR with the forward primer of the STS33 and the reverse primer of the STS43 generated a product of ~1.5 kb. The specific junction is showed by electrophoregram of part of the 734-bp sequence generated by junction-specific PCR with the primers JONCTION-U and JONCTION-L.

wild-type (WT) allele being too large (7.6 Mb) to be amplified (Figure 2).

It is noteworthy that the centromeric and telomeric breakpoints are located within two SINEs (short interspersed nucleotide elements), a 305 bp ALUSx and a 47 bp MIRb (mammalian-wide interspersed repeat type b), respectively. As an uncommon ALU-mediated *NF1* microdeletion has previously been reported, our findings support a role of these interspersed repeated structures in rearrangements leading to large deletions.[11] However, no significant overlap was found between these two sequences, suggesting nonhomologous end joining (NHEJ) as the likely involved mechanism.[9]

The deletion included the entire *NF1* locus and approximately 100 other genes, including numerous chemokine genes and four microRNA genes (Supplementary Figure 1).

Interestingly, the centromeric breakpoint was located in intron 4 of the *PIPOX* gene (pipecolic acid oxidase; NM_016518) and the telomeric breakpoint in intron 5 of the *GGNBP2* gene (gametogenetin-binding protein 2; NM_024835) coding a transcription factor (Figure 3a). *PIPOX* encodes a human peroxisomal enzyme (similar to the monomeric sarcosine oxidases) essential for the degradation of L-pipecolic acid.[12] While little experimental information exists, *GGNBP2* could be involved in a process associated with spermatogenesis but might also have a tumor suppressive activity (*GGNBP2* is also known as *LCRG1* for *laryngeal carcinoma-related gene 1*).[13,14] As *PIPOX* and *GGNBP2* have the same transcriptional orientation, we suspected the production of a chimeric transcript. We successfully amplified and sequenced this transcript in the propositus, with primers CHIMERIC-U/L designed to hybridize to *PIPOX* exon 4 and *GGNBP2* exon 6, respectively (Figure 3b). We then quantified the chimeric *PIPOX/GGNBP2* transcript, and the two WT *PIPOX* and *GGNBP2* transcripts, in lymphocytes from the propositus and from five healthy controls (Figure 4). The chimeric *PIPOX/GGNBP2* transcript was detected exclusively in the propositus, at an expression level ($C_t = 29$) similar to that of the *GGNBP2* transcript. It is noteworthy that the WT *PIPOX* transcript was not expressed ($C_t > 35$) in healthy control leukocytes, whereas its expression seemed to be reactivated in the propositus.

Discussion

The purpose of this study was to identify the genetic abnormality responsible for a peculiarly severe NF1

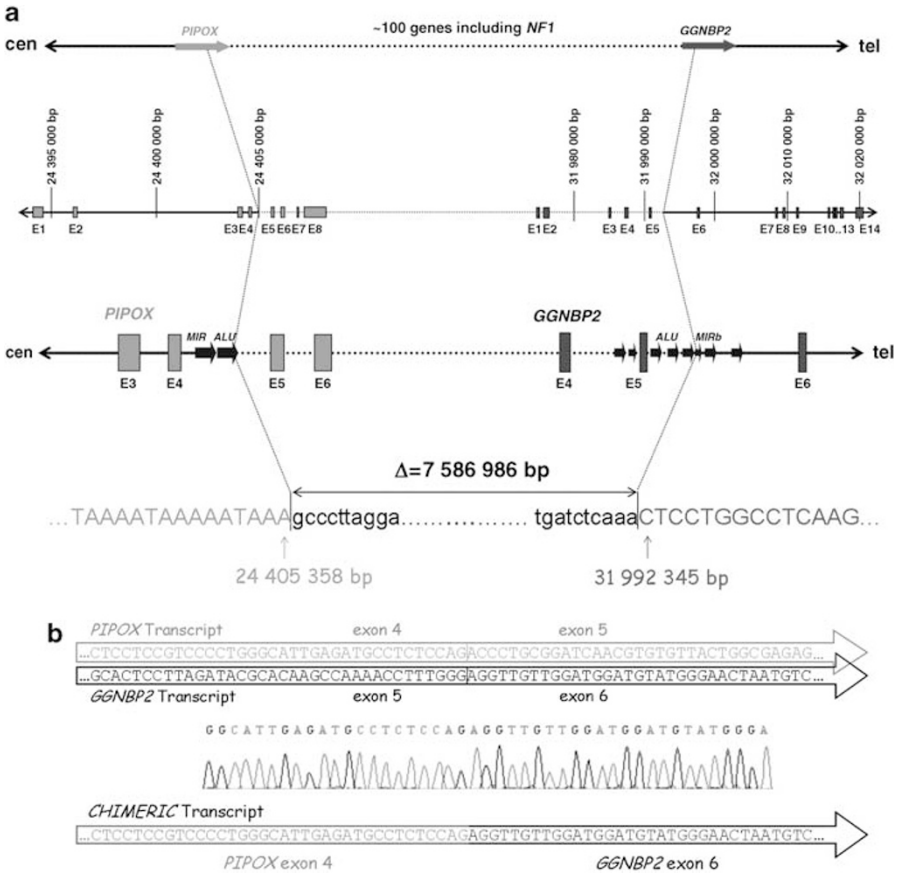

Figure 3 (**a**) Breakpoints of the genomic deletion. The centromeric and telomeric breakpoints are located in intron 4 of the *PIPOX* gene and in intron 5 of the *GGNBP2* gene, respectively. Both breakpoints are within SINE elements. (**b**) Electrophoregram of part of the chimeric transcript sequence, showing the specific junction. The chimeric transcript sequence was amplified and sequenced with forward and reverse primers designed to hybridize to *PIPOX* exon 4 and *GGNBP2* exon 6, respectively.

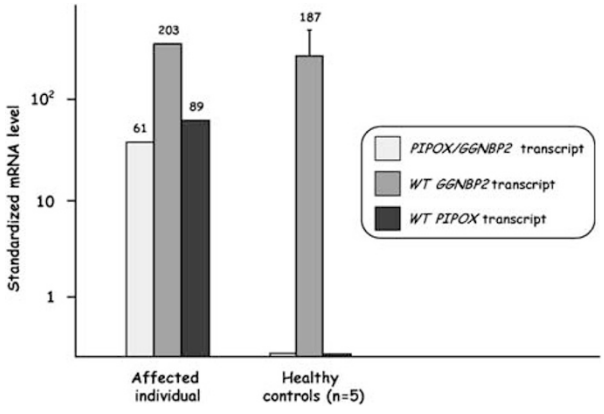

Figure 4 Quantification of the chimeric *PIPOX*/*GGNBP2* transcript, and the two wild-type (WT) *PIPOX* and *GGNBP2* transcripts by real-time RT-PCR from lymphocytes of the patient and of five healthy controls. The primer pairs for WT *PIPOX* and *GGNBP2* transcripts were selected to be specific for the WT transcripts, without the amplification of the chimeric *PIPOX*/*GGNBP2* transcript. For each gene, the mRNA level was normalized such that the 'basal mRNA level' was 1. The *GGNBP2* mRNA level in the healthy controls is the mean (± SEM) for the five individuals.

phenotype in a French patient who also had several other abnormalities not classically related to NF1. By applying STS real-time PCR-based gene-dose mapping to the affected family, we identified a 7.6-Mb germline deletion encompassing the entire *NF1* locus and approximately 100 other genes. This large, atypical deletion of the *NF1* locus was compatible with the classical NF1-related disorders observed in the patient.[6] The unusual phenotype might be due to (i) coincidental occurrence of the *NF1* microdeletion and a second genetic alteration at another locus; or (ii) a contiguous gene syndrome caused by haploinsufficiency of the *NF1* gene and of one or several additional genes within the 7.6 Mb deletion.

As the propositus had several features reminiscent of the Noonan syndrome (characteristic craniofacial anomalies, pterygium colli, and pulmonary valve stenosis; NS, OMIM 163950), we sought a *de novo* mutation in known NS culprit genes. NS is a heterogeneous genetic condition caused by autosomal dominant gain-of-function mutations in *PTPN11* (encoding SHP-2) at 12q24,[15] and more rarely, in *SOS1* at 2p22-p21,[16] *KRAS* at 12p12,[17] and *RAF1* (alias

CRAF) at 3p25.[18] Germline mutations of *PTPN11, RAF1, SOS1*, and *KRAS* have been identified in respectively ~50, ~15, ~10 and <5% of individuals with NS. In addition, NF1 and NS have previously been found to coexist in the same patient.[19] No *PTPN11, KRAS, RAF1*, or *SOS1* coding-sequence mutations were found in the reported patient. However, mutations of these four genes account for only about 80% of NS cases, meaning that we cannot formally rule out the co-occurrence of NS and NF1 in the reported patient, despite our extensive molecular studies.

NF1 patients with *NF1* microdeletions that encompass the entire coding region and neighboring genes often have a more severe phenotype, and atypical manifestations, than patients with intragenic *NF1* mutations, supporting the existence of a contiguous gene syndrome.[20] The severe and atypical phenotype is characterized by earlier onset, more neurofibromas, cognitive defects, variable dysmorphic features (prominent forehead, ptosis, down-slanted palpebral fissures, hypertelorism, short nose, low-set ears, micrognathia, and general facial coarsening), cardiac anomalies, and an increased risk of peripheral nerve-sheath malignancies.[20,21] The extreme variability of the *NF1* microdeletion syndrome and the small number of deletions so far characterized (fewer than 20 atypical *NF1* deletions) mean that genotype–phenotype correlation studies are often inconclusive.[8] The recurrent microdeletions previously described in individuals with NF1 span 1.4 and 1.2 Mb and encompass, in addition to *NF1*, 13 and 12 genes, respectively. On the basis of gene expression patterns and functions, it has been proposed that haploinsufficiency of *OMG* (oligodendrocyte myelin glycoprotein; NM_002544) could be involved in the mental retardation seen in patients with large *NF1* microdeletions.[20] Regarding the cardiovascular malformations observed in this setting, *SUZ12* and *CENTA2* (centaurin, alpha 2; NM_018404) have been considered as plausible culprit genes.[20] Recently, *RNF135* (ring-finger protein 135; NM_032322) haploinsufficiency has been shown to contribute to the phenotype in cases of *NF1* microdeletion.[22] The atypical non-NF1 abnormalities in the reported patient, and particularly the severe developmental and mental retardation, could result from haploinsufficiency of one or more of the additional genes specifically removed by her 7.6 Mb deletion (*versus* the 13 or 12 genes deleted in typical recurrent *NF1* microdeletions). Other large atypical *NF1* deletions have been characterized so far, in particular one approximately 7 Mb long deletion containing 60–240 genes without molecular identification of end points,[23] and a shorter 3 Mb deletion with junction fragment cloned.[9] Interestingly, the 7-Mb deletion carrier shared uncommon NF1 symptoms with the patient herein described (distinct craniofacial dysmorphisms, congenital heart defect, epileptic seizures, and severe mental retardation).[23] It is noteworthy that the deletion in the reported patient included a cluster of chemokine genes (*CCL1, 2, 3, 5, 7, 8, 11, 12, 13, 15, 16, 18, and 23*) and four microRNA genes (*hsa-mir-423, -193a, -365-2,* and *-632*), deletion of which may contribute to the atypical phenotype. Interestingly, using a new literature-mining bioinformatics approach to prioritize disease genes, based on aGeneApart software, we identified *NUFIP2* (nuclear fragile X mental retardation protein interacting protein 2; NM_020772) as a gene whose deregulation might be involved in the reported patient's mental retardation, being statistically associated with mental retardation in MEDLINE abstracts ($P<10^{-5}$). This gene encodes an 82-kD protein (called 82-FIP) distributed in various regions of the brain and interacting with FMR1 (encoded by *FMR1* for fragile-X mental retardation 1; NM_002024), the absence of which causes the most common monogenic form of mental retardation, the fragile-X syndrome.[24] Like other FMR1-interacting proteins (FXR1, FXR2, CYFIP1, and CYFIP2), 82-FIP might have a role in the development of the nervous system and in cognitive function. In this respect, *FXR2*-null mice show some behavioral phenotypes.[25] Computationally predicted target sites for microRNAs in *NUFIP2* 3′ UTR identified two potential binding sites for two miRNAs: *hsa-mir-873* and *hsa-mir-365-2*. Interestingly, *hsa-mir-365-2* (located between the *NF1* gene and *NF1-REP-c*) was deleted in the present reported patient. On the basis of these observations, and by analogy, we postulate that *NUFIP2* aberrations might be involved in the mental retardation or cognitive impairment observed in the reported patient.

Finally, we also identified a chimeric *PIPOX/GGNBP2* transcript resulting from the genomic deletion. It showed marked expressed relative to WT *PIPOX* and *GGNBP2* transcripts. Computational translation (starting at the *PIPOX* translation initiation codon) yielded a shorter protein (236 amino acids) owing to a premature stop codon (the *GGNBP2* open reading frame was not conserved). This chimeric transcript and/or the fusion protein might also contribute to the patient's phenotype, even if chimeric transcripts have exceptionally been described in constitutional pathology.[26] WT *PIPOX* allele reactivated expression in the propositus leukocytes suggested a complex molecular mechanism (ie, involvement of a nonidentified noncoding RNA).

Further studies will be necessary to identify the putative fusion protein and to define the role of the chimeric transcript and/or the ~100 deleted genes in this severe phenotype. These studies should initially focus on the chemokine gene cluster, the microRNA genes, and the *NUFIP2* gene deregulation. A large series of *NF1* microdeleted patients also need to be genotyped (with molecular identification of each end point) and phenotyped in detail (with attention to uncommon NF1 features) to detect a possible correlation between alteration of specific genes adjacent to *NF1* and particular clinical features.

Acknowledgements

We thank the patients and their parents for participation. This work was supported in part by grants from the Association Neurofibromatoses et Recklinghausen. We are also grateful to KU LEUVEN R&D as the provider of aGeneApart.

References

1 Carey JC, Baty BJ, Johnson JP, Morrison T, Skolnick M, Kivlin J: The genetic aspects of neurofibromatosis. *Ann N Y Acad Sci* 1986; **486**: 45–56.
2 Ferner RE, Huson SM, Thomas N *et al*: Guidelines for the diagnosis and management of individuals with neurofibromatosis 1. *J Med Genet* 2007; **44**: 81–88.
3 Radtke HB, Sebold CD, Allison C, Haidle JL, Schneider G: Neurofibromatosis Type 1 in Genetic Counseling Practice: Recommendations of the National Society of Genetic Counselors. *J Genet Couns* 2007; **16**: 387–407.
4 Xu GF, O'Connell P, Viskochil D *et al*: The neurofibromatosis type 1 gene encodes a protein related to GAP. *Cell* 1990; **62**: 599–608.
5 Kluwe L, Siebert R, Gesk S *et al*: Screening 500 unselected neurofibromatosis 1 patients for deletions of the NF1 gene. *Hum Mutat* 2004; **23**: 111–116.
6 Steinmann K, Cooper DN, Kluwe L *et al*: Type 2 NF1 deletions are highly unusual by virtue of the absence of nonallelic homologous recombination hotspots and an apparent preference for female mitotic recombination. *Am J Hum Genet* 2007; **81**: 1201–1220.
7 Raedt TD, Stephens M, Heyns I *et al*: Conservation of hotspots for recombination in low-copy repeats associated with the NF1 microdeletion. *Nat Genet* 2006; **38**: 1419–1423.
8 Mantripragada KK, Thuresson AC, Piotrowski A *et al*: Identification of novel deletion breakpoints bordered by segmental duplications in the NF1 locus using high resolution array-CGH. *J Med Genet* 2006; **43**: 28–38.
9 Venturin M, Gervasini C, Orzan F *et al*: Evidence for non-homologous end joining and non-allelic homologous recombination in atypical NF1 microdeletions. *Hum Genet* 2004; **115**: 69–80.
10 Bieche I, Parfait B, Le Doussal V *et al*: Identification of CGA as a novel estrogen receptor-responsive gene in breast cancer: an outstanding candidate marker to predict the response to endocrine therapy. *Cancer Res* 2001; **61**: 1652–1658.
11 Gervasini C, Venturin M, Orzan F *et al*: Uncommon Alu-mediated NF1 microdeletion with a breakpoint inside the NF1 gene. *Genomics* 2005; **85**: 273–279.
12 Dodt G, Kim D, Reimann S, McCabe K, Gould SJ, Mihalik SJ: The human L-pipecolic acid oxidase is similar to bacterial monomeric sarcosine oxidases rather than D-amino acid oxidases. *Cell Biochem Biophys* 2000; **32**: 313–316.
13 Zhang J, Wang Y, Zhou Y, Cao Z, Huang P, Lu B: Yeast two-hybrid screens imply that GGNBP1, GGNBP2 and OAZ3 are potential interaction partners of testicular germ cell-specific protein GGN1. *FEBS Lett* 2005; **579**: 559–566.
14 Li Y, Chen Z: Molecular cloning and characterization of LCRG1 a novel gene localized to the tumor suppressor locus D17S800-D17S930. *Cancer Lett* 2004; **209**: 75–85.
15 Tartaglia M, Kalidas K, Shaw A *et al*: PTPN11 mutations in Noonan syndrome: molecular spectrum, genotype-phenotype correlation, and phenotypic heterogeneity. *Am J Hum Genet* 2002; **70**: 1555–1563.
16 Roberts AE, Araki T, Swanson KD *et al*: Germline gain-of-function mutations in SOS1 cause Noonan syndrome. *Nat Genet* 2007; **39**: 70–74.
17 Schubbert S, Zenker M, Rowe SL *et al*: Germline KRAS mutations cause Noonan syndrome. *Nat Genet* 2006; **38**: 331–336.
18 Razzaque MA, Nishizawa T, Komoike Y *et al*: Germline gain-of-function mutations in RAF1 cause Noonan syndrome. *Nat Genet* 2007; **39**: 1013–1017.
19 Bertola DR, Pereira AC, Passetti F *et al*: Neurofibromatosis-Noonan syndrome: molecular evidence of the concurrence of both disorders in a patient. *Am J Med Genet* 2005; **136**: 242–245.
20 Venturin M, Guarnieri P, Natacci F *et al*: Mental retardation and cardiovascular malformations in NF1 microdeleted patients point to candidate genes in 17q11.2. *J Med Genet* 2004; **41**: 35–41.
21 De Raedt T, Brems H, Wolkenstein P *et al*: Elevated risk for MPNST in NF1 microdeletion patients. *Am J Hum Genet* 2003; **72**: 1288–1292.
22 Douglas J, Cilliers D, Coleman K *et al*: Mutations in RNF135, a gene within the NF1 microdeletion region, cause phenotypic abnormalities including overgrowth. *Nat Genet* 2007; **39**: 963–965.
23 Upadhyaya M, Roberts SH, Maynard J *et al*: A cytogenetic deletion, del(17)(q11.22q21.1), in a patient with sporadic neurofibromatosis type 1 (NF1) associated with dysmorphism and developmental delay. *J Med Genet* 1996; **33**: 148–152.
24 Bardoni B, Castets M, Huot ME *et al*: 82-FIP, a novel FMRP (fragile X mental retardation protein) interacting protein, shows a cell cycle-dependent intracellular localization. *Hum Mol Genet* 2003; **12**: 1689–1698.
25 Bontekoe CJ, McIlwain KL, Nieuwenhuizen IM *et al*: Knockout mouse model for Fxr2: a model for mental retardation. *Hum Mol Genet* 2002; **11**: 487–498.
26 Borsani G, Piovani G, Zoppi N *et al*: Cytogenetic and molecular characterization of a de-novo t(2p;7p) translocation involving TNS3 and EXOC6B genes in a boy with a complex syndromic phenotype. *Eur J Med Genet* 2008, doi: 10.1016/j.ejmg.2008.02.006 (in press).

Supplementary Information accompanies the paper on European Journal of Human Genetics website (http://www.nature.com/ejhg)